

Thrust Losses in Hypersonic Engines Part 2: Applications

D. W. Riggins*

University of Missouri–Rolla, Rolla, Missouri 65409

The methodology developed in Part 1 of this investigation (Riggins, D. W., McClinton, C. R., and Vitt, P. H., "Thrust Losses in Hypersonic Engines Part 1: Methodology," *Journal of Propulsion and Power*, Vol. 13, No. 2, 1997, pp. 281–287) for the identification and evaluation of the thrust losses in a scramjet engine is applied to one-dimensional scramjet engine flows with coupled loss mechanisms. Thrust and thrust potential losses are related directly to increases in irreversible entropy caused by friction, heat transfer, mixing, nonequilibrium reaction, and shocks. This method is extended to enable the evaluation of thrust losses in multidimensional flows. The fundamental relationship between performance assessment utilizing multidimensional flowfields and cycle analysis performance prediction is shown and discussed.

Introduction

THE successful development of air-breathing propulsion systems for high-speed aerospace vehicles requires the rational optimization of engine thermofluid dynamic characteristics. Because of the integration of the propulsion system and the airframe necessary for achieving high Mach number flight, overall mission-oriented optimization of a hypersonic vehicle can strongly influence many design features of the propulsion system. However, even within the context of vehicle and mission constraints, the primary function of an air-breathing propulsion system designed for any speed regime is the effective utilization of the onboard fuel to deliver adequate thrust for achieving both acceleration and cruise requirements of the mission. Therefore, identifying mechanisms that cause reductions in the ability of a propulsion system to deliver thrust and quantifying the thrust losses associated with these mechanisms are of critical importance in the design and evaluation of high-speed engines. This investigation focuses on demonstrating the application of the methodology developed in the companion paper for describing and evaluating thrust losses resulting from flow irreversibilities within the propulsion flow paths of supersonic combustion ramjet engines (scramjets). However, the methods and techniques described in this investigation are useful for any Brayton cycle aerospace engine, including ramjets and engines with turbomachinery.

The specific purposes of this investigation are to first demonstrate the application of the one-dimensional method for quantifying thrust losses caused by irreversibilities and then to extend the application of the method to multidimensional propulsive flowfields. Irreversibilities are manifested by associated increases in entropy or, equivalently, by reductions in work availability as measured from some reference condition. Therefore, the irreversible entropy increase associated with a real thermofluid dynamic process is a measure of how far (in terms of reduced potential for delivering work) that process is from the completely reversible process, i.e., the process that would (potentially) deliver the maximum work for the same heat input. Since the useful work of an aerospace jet engine is the thrust work delivered by the engine to the vehicle, it is necessary to define the flow losses of the actual irreversible engine as losses in delivered thrust work as measured from the thrust work of the reversible engine. In addition to the reversible engine, an ideal engine can also be defined; such an engine is

both reversible and has maximum (complete) heat release. The thrust loss of the reversible engine as measured from the ideal engine then defines the thrust loss caused by incomplete heat release (or combustion). Based on these observations, the companion paper of this investigation¹ develops a method for directly calculating the lost thrust work in an actual engine in terms of the irreversible entropy increases and incomplete combustion.

Previous applications work in the area of the second-law analysis of jet engines includes that of Clarke and Horlock,² who utilized standard availability concepts to analyze a turbojet. Lewis³ discussed the propulsive efficiency and its relationship to energy availability and observed the inevitable difference in application between standard energy availability and obtainable thrust work (even for the ideal engine). Riggins et al.⁴ performed a computational investigation in which they assessed optimal combustor length in three-dimensional scramjet combustor simulations by measuring the axial distribution of the maximum thrust work availability by isentropic expansion to a reference condition (fixed area or pressure). This procedure (utilizing a fixed area) for evaluating thrust work potential in a flow is also used in this work for the presentation of some of the results. Murthy⁵ discusses the method of applying standard exergy (available work) concepts to a scramjet engine; reductions in work availability measured from ambient conditions are computed in a straightforward manner utilizing the quantifiable irreversible entropy increases in the actual engine. Then, to relate the losses in exergy to the propulsive losses, an engine effectiveness parameter is defined as the ratio of thrust work losses to exergy losses.

This paper first presents a review and discussion of the method for evaluating lost thrust caused by irreversibilities within the context of quasi-one-dimensional streamtube theory. An application to a scramjet flowfield generated by a cycle-code is shown both in terms of distributions of raw engine stream thrust with stream thrust increments lost because of various loss mechanisms and in terms of engine stream thrust potential¹ distribution and stream thrust potential losses. As a demonstration of the parametric assessment of thrust loss contributions, a study of the effect of fuel temperature on thrust losses in a scramjet engine is reviewed. The focus in subsequent sections is on evaluating losses in multidimensional flows; fundamental issues involving multidimensional losses are discussed and the methodology for performing thrust loss calculations in such flows is developed. The resulting technique is first applied to an analytical (non-numerical) multidimensional flowfield to assess its reliability. The method is then applied to a complex multidimensional flowfield with friction, heat transfer, fuel–air mixing, and finite rate reactions and shocks. Results are shown in terms of flowfield structure,

Received July 14, 1995; revision received Aug. 5, 1996; accepted for publication Sept. 3, 1996. Copyright © 1996 by the American Institute of Aeronautics and Astronautics, Inc. All rights reserved.

*Associate Professor, Department of Mechanical and Aerospace Engineering. Member AIAA.

irreversibility distributions, and the lost thrust increments caused by various loss mechanisms within the flow.

Computation of Engine Performance Losses Caused by Flow Irreversibilities

A method for computing engine thrust losses caused by irreversibilities is developed in detail in the companion paper of this investigation.¹ This section provides a brief discussion of the application of this technique to aerospace engines. The method is based upon the observation that the lost thrust work as measured from that of the reversible engine is recoverable (and, hence, is able to be quantified) by an additional isentropic expansion of the nozzle exit flowfield (see Fig. 1). The analysis utilizes quasi-one-dimensional streamtube theory and the second law of thermodynamics to fully describe the flow through an aerospace engine. The additional nozzle expansion necessary to recover the lost thrust is derived in terms of the irreversible entropy gain as follows:

$$A_{er}/A_e = \exp(\Delta S_{ir}/R)$$

Here, A_e is the nozzle exit area, A_{er} is the area that the flow must be isentropically expanded to quantify the lost thrust associated with the irreversible entropy increase ΔS_{ir} , and R is the gas constant. The expansion process is shown in the companion paper of this investigation to describe a stream thrust-equivalent family of engines with irreversibilities progressively removed from nozzle exit to inlet entrance, such that the exit stream thrust of the completely reversible engine is exactly recovered at the end of the expansion process. This analytical technique for recovering stream thrust lost because of irreversibilities in a flowfield then enables the direct calculation of the magnitude of the lost net thrust. The concept is readily extended to deal with flows with coupled losses, i.e., losses that are concurrent and interact with one another through the local flow conditions. This extension to include coupled losses is possible as long as a detailed differential description of the flow irreversibilities is provided. The technique of additional expansion for quantifying thrust losses can then be applied, moving differentially (from nozzle exit to inlet entrance) along the thermodynamically consistent path of recovering stream thrust losses. Thrust losses associated with individual loss mechanisms (friction, heat transfer, nonequilibrium kinetics, mixing, or shocks) can be specifically assessed. However, because coupling between mechanisms is implicitly included within the calculated entropy changes, the magnitude of a thrust loss caused by a specific mechanism cannot be considered as independent of the thrust losses because of the other loss mechanisms.

The method also allows the direct quantitative assessment of mixing enhancement techniques in scramjet combustors. Such techniques usually rely on geometry or flow variation to

enhance mixing and heat release. Because of the inevitable generation of irreversible entropy (i.e., flow losses) by the use of these techniques, there exists a critical balance between the generated irreversibility (which adversely affects engine performance), and the performance benefit of increased combustion. Mixing enhancement techniques have typically been assessed in terms of mixing/combustion efficiency; they are also occasionally presented along with the total pressure drop (i.e., the irreversible entropy gain) associated with the mixing enhancement scheme. To date, however, there has been no reliable technique for rigorously relating the two phenomena from the standpoint of performance assessment. The method described in this investigation, however, enables the direct computation of the thrust losses caused by irreversibility and the thrust losses caused by incomplete combustion and should provide a useful design tool in the development of practical mixing enhancement strategies for high-speed engines.

Thrust Losses in Scramjet Engines (Cycle Code Results)

The previous section reviewed the background of a streamtube-based method for evaluating thrust losses caused by various irreversibilities in jet engines. This section summarizes an application of this technique to a cycle code generated flowfield for a scramjet configuration and provides a discussion on the relationship between the actual stream thrust losses throughout the engine (computed using the method described in the previous section) and the related stream thrust potential¹ losses utilizing the same method.

Figure 2 is a schematic of the engine geometry that has been selected for consideration in this section. Inflow and injection conditions are as specified in this figure. This example is not an optimized configuration but is defined only to be representative of general scramjet flows for a Mach 12 flight condition. The one-dimensional cycle code developed in this work is fully described in the companion paper¹; the code is a standard cycle solver with finite rate H_2-O_2 reaction capability. It has, however, been written with detailed attention given to both second-law accounting (i.e., the computation of irreversibilities caused by loss mechanisms) and associated performance loss assessment. This code assumes instantaneous mixing of the airstream and the fuel stream at the location of injection; incomplete combustion results from finite rate reactions within the mixed stream as the flow progresses down the combustor and into the nozzle. This simple treatment of the mixing process is not mandated by the thrust loss-performance method that is the focus of this work. This method can be readily applied to higher level cycle codes and, as will be shown in subsequent sections in this paper, to multidimensional flowfields as well.

Actual stream thrust ($\dot{m}U + PA$) vs axial distance is plotted in Fig. 3; this quantity corresponds to the bottom curve in this figure. The actual stream thrust declines in the inlet because of the fluid dynamic compression (area decrease) and the action of friction. The magnitude of the net inlet drag can be

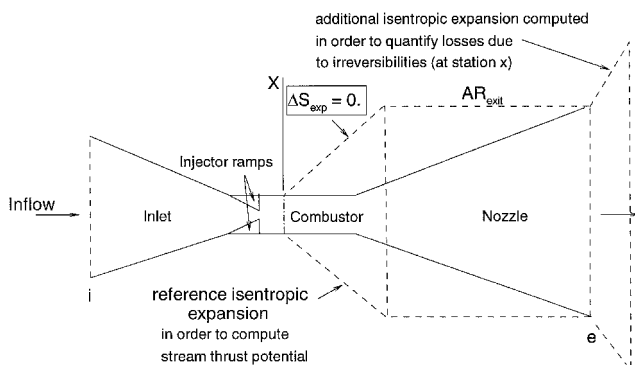


Fig. 1 Schematic of scramjet engine showing reference isentropic expansion to nozzle exit area and additional expansion to recover lost thrust caused by irreversibility.

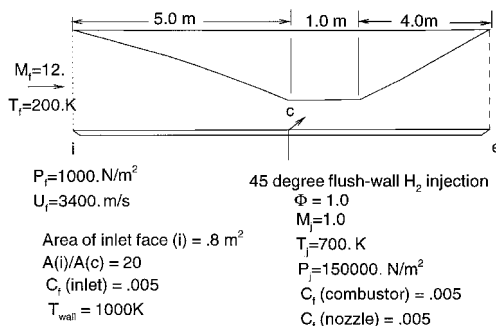


Fig. 2 Schematic of generic scramjet engine geometry used for cycle code studies.

obtained by simply subtracting the inflow stream thrust from the actual inlet exit stream thrust. Note that the stream thrust of the reversible engine (or the stream thrust of the actual engine with lost thrust work recovered) also declines in the inlet because of flow compression and wall cooling. The actual stream thrust in the combustor increases initially because of the downstream-directed component of fuel momentum at the injection location and then drops throughout the constant area section because of friction. In the nozzle ($X > 6$ m), the stream thrust increases because of nozzle expansion; it is only in this expansion region that any benefit of upstream combustion is realized in terms of increasing stream thrust. At the end of the nozzle, the flow stream thrust has barely reached the inlet stream thrust itself. This results in approximately zero net thrust for this (unoptimized) scramjet flowfield.

The region A + B + C in Fig. 3 represents the total stream thrust lost because of irreversibilities in the engine and is computed simply using the local area as the base area for the lost thrust recovery process discussed in the previous section. Region D represents the lost thrust caused by incomplete combustion. For this example, these results indicate (by examining the various stream thrust losses at the nozzle exit) that about 57% of the overall engine thrust effectiveness is lost because of incomplete combustion, 25% is lost because of friction, 8% because of finite rate reaction losses, and 10% because of fuel-air mixing and injection losses.

Figure 4 is based on the same flowfield analysis, except results are presented in terms of stream thrust potential using the nozzle exit area as the reference area, i.e., the local flow is isentropically expanded to the nozzle exit area before the lost thrust recovery method is performed (see Fig. 1). In the inlet, from the standpoint of thrust potential, the reversible flow can always be returned (expanded) to the inlet area (equal in this example to the nozzle exit area) with no loss in stream thrust caused by irreversibilities. Thus, any loss in the thrust potential of the ideal engine through the inlet is a result only of wall heat removal. Hence, the rationale for showing earlier results in terms of actual stream thrust throughout the engine (Fig. 3) is to demonstrate that the method of recovering lost stream thrust work and, hence, quantifying losses, can be performed on the local flow (utilizing the local cross-sectional area) with no thrust potential issues involved. Significantly, at the nozzle exit, the stream thrust potential and associated thrust potential losses are exactly equal to the associated actual stream thrusts (by inspection of Figs. 3 and 4 and by definition of the thrust potential parameter). Hence, reductions in overall engine thrust effectiveness caused by flow losses are equivalent whether examining raw stream thrust or stream thrust potential.

The effect on engine thrust production of varying fuel temperature at constant fuel equivalence ratio in a similar geometry with the same inflow conditions is shown in Fig. 5. For

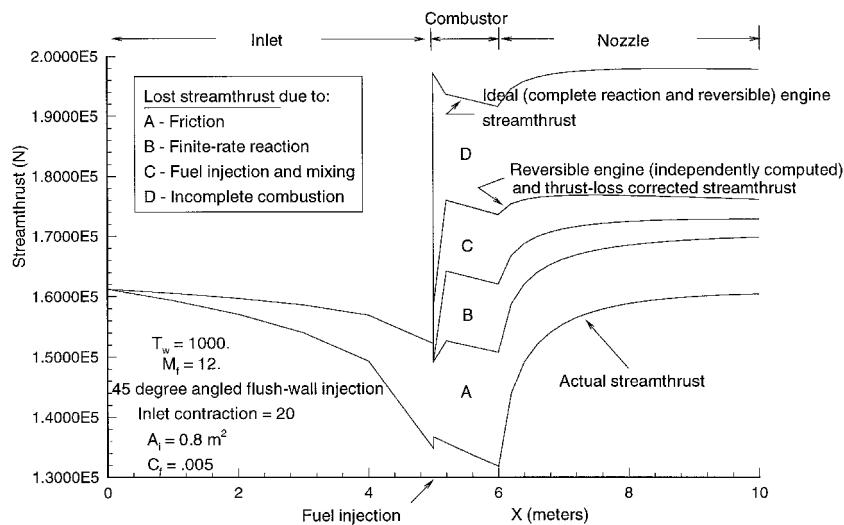


Fig. 3 Stream thrust and lost stream thrust vs axial distance through generic scramjet engine.

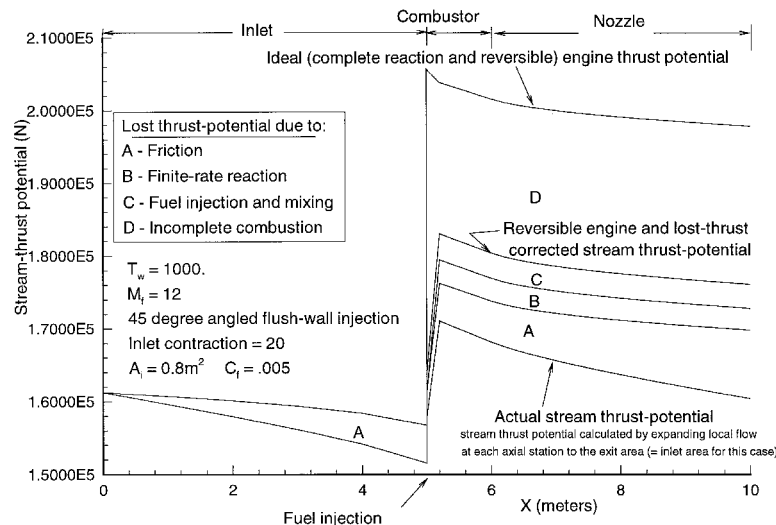


Fig. 4 Stream thrust potential and lost stream thrust potential vs axial distance through generic scramjet engine.

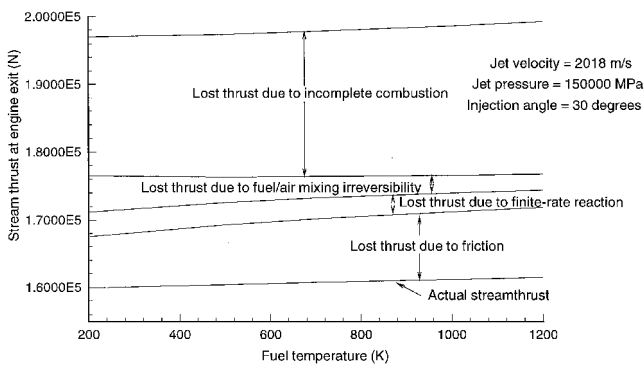


Fig. 5 Effect of fuel temperature on thrust losses in a scramjet engine.

this case, the fuel injection angle is chosen as 30 deg (directed downstream). This figure plots fuel temperature vs computed stream thrust at the engine exit with thrust losses caused by various loss mechanisms shown as increments above the actual stream thrust (bottom curve). The actual stream thrust increases because of increasing fuel temperature. The difference, however, is slight in terms of gross stream thrust. The lost thrust increment caused by the fuel/air mixing irreversibility is seen to decrease significantly with increasing fuel temperature. This is because of lower temperature gradients between the (hot) air and the (cooler) fuel within the mixing region. The thrust loss associated with irreversibilities caused by finite rate reaction also drops slightly with increasing fuel temperature because of the higher bulk temperature after mixing. The same effect increases the thrust loss caused by friction (because of more heat transfer between the flow and the wall, which is held at 1000 K). These one-dimensional results utilizing the thrust loss recovery method demonstrate its potential for diagnosing engine performance and for assisting in injector design and evaluation.

Irreversibilities in Multidimensional Flowfields

The preceding sections describe the development and application of a technique for the systematic evaluation of thrust losses. These losses are caused by flow-generated irreversibilities and are measured in terms of reductions in either local stream thrust or stream thrust availability, i.e., the thrust obtained by expanding the local flow isentropically to a reference area. The analysis is developed from the standpoint of quasi-one-dimensional flow (flow in a variable-area streamtube) with friction, convective heat transfer, fuel injection and mixing (mass, momentum, and energy addition), and nonequilibrium reaction. To be useful for analyzing numerical computational fluid dynamics (CFD) solutions, this methodology for evaluating thrust lost caused by individual loss mechanisms must be extended to multidimensional flows, in which there are multiple adjacent and interacting streamtubes. These streamtubes are bundled together within an aerospace engine flowfield such as to form the primary (or overall) engine flow-path streamtube. Within this primary streamtube, each secondary streamtube works on or is worked upon by adjacent streamtubes and/or system boundaries through the action of viscosity. This process simply represents momentum transfer from higher velocity streamtubes to lower velocity streamtubes, usually culminating in wall shear stresses and the associated frictional drag on the flow at the boundaries of the wall-bounded streamtubes. Similarly, heat is transferred from hotter to cooler streamtubes within the flow. For flow in the vicinity of an adiabatic wall, this mechanism results in a continuous flow of heat into the outer flow, away from the wall region. This heat has its source in the friction-driven transfer of directed kinetic energy into internal energy within the low-velocity near-wall region. For a cold wall, heat flows into the wall itself as well as into the outer flow, away from the inner boundary-layer

region. Finally, mass transfer by diffusion can also take place between neighboring streamtubes. This process is driven by variations in species composition. In a real flow, all three transfer mechanisms (mass, momentum, and energy transfer) between adjacent streamtubes or boundaries have associated and quantifiable increases in irreversibility.

In addition to irreversibilities caused by transfer mechanisms between adjacent streamtubes (or with the system boundaries), there can also be the production of irreversible entropy within the flow caused by finite rate reactions and the presence of shock waves. In actuality, the irreversibility associated with a shock is caused by the large gradients in momentum and energy through the shock structure itself. Hence, a Navier-Stokes simulation with grid resolution adequate enough to capture the internal shock structure would automatically incorporate the shock irreversibility within the context of explicitly computed transfer mechanisms between adjacent streamtube sections (located within the shock layer). However, it is rarely practical or desirable to obtain multidimensional numerical simulations that adequately resolve inner shock structure; hence, for shock prediction, numerical simulations usually rely on the implicit entropy jump permissible within the context of Euler equations (which are essentially the multidimensional representation of the Rankine-Hugoniot one-dimensional relations). This is also partially true for full Navier-Stokes simulations as well, since the Euler equations are simply a subset of the Navier-Stokes equations. However, in a Navier-Stokes simulation of a complex flow, a portion of the shock-induced irreversibilities may, in fact, be captured by the computations involving the transfer mechanisms between adjacent streamtubes. This is because of shock spreading across cells (or streamtubes) caused by physically modeled diffusion processes. In general, the flow losses caused by particular loss mechanisms are both cumulative and coupled:

- 1) The flow in a streamtube at a given station is dependent on the complete loss history upstream of that station.
- 2) Since each local loss affects the local flow condition, which in turn affects the loss mechanism itself, the individual losses are then coupled with each other via the local flow conditions.

It is important to note that, although the second law demands that the overall cumulative irreversible entropy must increase throughout the flow, it is possible that, in a flow with coupled losses, an individual cumulative entropy (associated with a particular mechanism) can actually decrease. A simple example of this phenomena is convective heat transfer from a fluid to a cold wall (through a boundary layer). The convective heat transfer results in an increase in total pressure, although the associated (coupled) frictional total pressure drop is always such that the total irreversibility increases.

Thrust Modeling Methodology for Multidimensional Flows

It is conceptually easy to envision the straightforward application of the lost-thrust method (as previously developed for a single streamtube) by analyzing each streamtube separately within a given multidimensional flow. Consider, as an example, flow with uniform axial inflow in which the complete spatial differential description of all irreversibilities and streamtube locations and shapes are known at given axial planes out to some specified exit plane. It is possible, then, to separately compute the thrust losses for each streamtube using the lost thrust work recovery technique described earlier and then to sum the results across the streamtubes at the exit of the flow. Note that to account for flow angularity each streamtube is isentropically turned into the axial direction at the axial position of interest (before the lost thrust increments at that position are computed). This is done since the base area associated with quantifying the lost thrust is the cross-sectional area of the streamtube and the calculation of the lost thrust is most usefully referenced in the axial direction. For evaluation

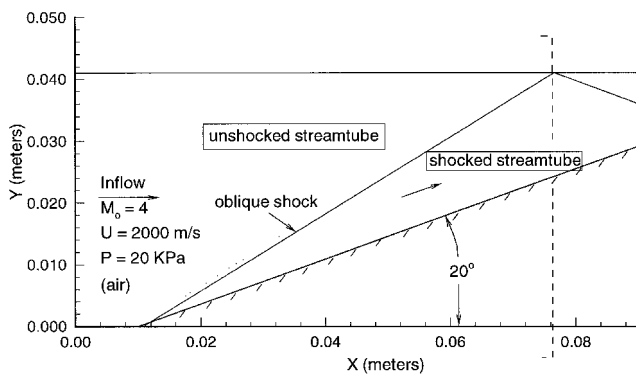


Fig. 6 Schematic for analytical oblique shock flowfield; used for application of lost thrust methodology to multidimensional flow-field.

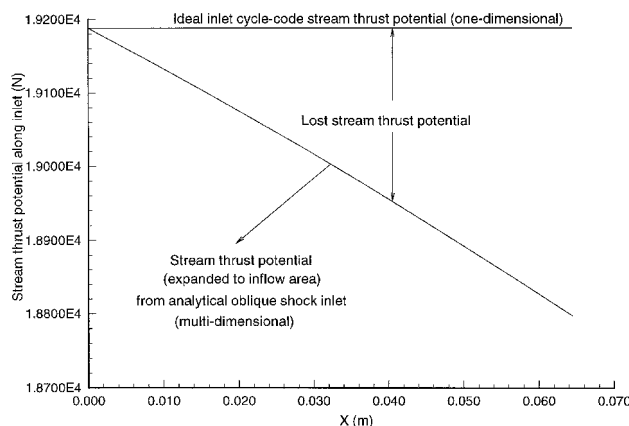


Fig. 7 Stream thrust potential and lost stream thrust potential for oblique shock flowfield.

of the thrust potential (if desired), the exit area for the local reference isentropic expansion before the loss evaluation for each streamtube would be determined by the ratio of the individual streamtube mass-flow rate to the overall mass-flow rate and by the desired overall reference area (most usefully the actual nozzle exit area).

This procedure for analyzing multidimensional flows can be demonstrated for a simple analytic oblique shock problem as shown in Fig. 6, in which the inviscid oblique shock relations are used to generate a simple flowfield composed (at any given axial location) of a lower (shocked) streamtube and an upper (unshocked) streamtube. The shocked streamtube experiences a pointwise irreversibility increase at the station at which it traverses the shock. Since this multidimensional flowfield is completely analytical, there are no numerical or grid issues involved (i.e., CFD or modeling issues), and the merit of the previous approach for thrust modeling of multidimensional flows can be rigorously examined.

Figure 7 demonstrates the results of applying the technique discussed earlier to the analytical oblique shock flowfield. These results are shown in terms of stream thrust potential or stream thrust availability referenced to the inflow area itself. The flow is first analyzed at selected axial stations by expanding the two separate streamtubes independently and isentropically to the reference areas associated with their respective mass flow rates (after turning the shocked streamtube isentropically back into the axial direction, this involves an area change for that streamtube). The lost thrust caused by the shock is then computed or recovered by an additional isentropic expansion of the shocked streamtube, as detailed in previous sections. The resultant stream thrusts for the two streamtubes are then added together. This procedure returns the inflow stream thrust as shown in Fig. 7.

Although the method outlined earlier yields exact results for the case of a flowfield with constant total enthalpy, a more general method can be developed. This general method also does not require the tracking of each individual streamtube and its associated loss history from the inflow to the station of interest. Typical numerical simulations rely on spatial grids, which do not, in general, define coherent streamtube surfaces, i.e., the tracking of a single streamtube and its losses (irreversible entropy increases) from inflow to exit is, at best, a very difficult interpolation problem fraught with numerical issues. Instead, it is possible to mix the local streamtubes as defined by the local grid at a given axial station to define the equivalent overall engine streamtube. If done isentropically, such a thermodynamically permissible process fully preserves the inherent work availability that exists between streamtubes at different enthalpies. In the simple oblique shock example discussed earlier, the two streamtubes are appropriately mixed by turning the shocked streamtube into the axial direction isentropically and then performing an isentropic mixing process on the two streamtubes. The resulting one-dimensional flow can then be expanded to the inflow area and an additional nozzle expansion performed that corresponds to the recovery of the lost thrust work caused by the irreversible shock-induced entropy gain. The results of applying such a technique are identical to those for the previously defined method as shown in Fig. 7. This procedure eliminates entirely the need to track individual streamtubes and their losses from inflow to exit; the individual irreversibilities can be computed cellwise and then summed over the axial grid spacings using the CFD grid in a straightforward manner. This second-law distribution is then used to provide the lost thrust increments caused by the various mechanisms based now on the overall engine streamtube, just as done in the single streamtube cycle-code examples shown earlier. Note also that, in the general case, any mixing process (whether irreversible or reversible) implies heat/work/mass transfer between streamtubes with varying total enthalpies. This can actually result in marginal increases in the mixed flow thrust potential over that of the separate (unmixed) flows for real (irreversible) mixing processes. This, in fact, occurs in turbofan engines in which the core and the secondary (fan) streams are mixed before the nozzle. The isentropic mixing process described here provides the second-law limit for that increase in thrust potential. Note that, if desired, an irreversible (rather than isentropic) mixing process could be utilized in this method. However, such a process has an inevitable (stepwise) increase in irreversible entropy with an attendant loss in thrust potential.

Relation Between Thrust Prediction in Multidimensional Flows and One-Dimensional Flows

It should be emphasized that the methods outlined here relate the multidimensional thrust performance (or the prediction of the local stream thrust) to the cycle code thrust performance or stream thrust prediction (computed for reversible flow with the same geometry). It is possible, then, to directly relate the actual predicted engine thrust/drag (or the local net thrust or drag anywhere in the flow) from a multidimensional flowfield to the ideal cycle code (one-dimensional) computed thrust for the same geometry and conditions. This becomes apparent when it is considered that the fundamental difference (other than grid and numerical issues) between a steady-state multidimensional Navier-Stokes simulation that has been one dimensionalized as suggested in the previous section and an ideal (reversible) cycle code simulation with the same total axial enthalpy schedule is a result only to the effect of flow losses (which are quantifiable in terms of performance as increments above the actual provided thrust).

Thrust Losses in a Multidimensional Scramjet Engine Flowfield

The following section describes the application of the method for evaluating lost thrust to a multidimensional scramjet engine flowfield. This application is performed by utilizing the technique described in the previous section.

A two-dimensional (subscale) scramjet geometry is defined that has a compression ramp (corresponding to an inlet) followed by a constant-area section (combustor) in which fuel is injected and burned (see Fig. 8). The inflow to the domain is Mach 5 air with a static temperature of 1066 K and static pressure of 50 KPa. A 1-cm flat plate region is included upstream of the compression ramp. The domain height at the inflow is 4.1 cm and the angle of the ramp is 10 deg. The overall inlet length (including the upstream section) is 0.1455 m. The length of the constant area combustor is 10 cm. Hydrogen is injected as shown at the shoulder of the inlet-combustor at a downstream-directed angle of 12 deg with a velocity of 3110 m/s and static temperature and pressure of 426 K and 150 KPa, respectively. The injector is sized such that the fuel equivalence ratio is approximately 1.0. The upper boundary is a reflection plane, whereas the lower boundary is treated as a no-slip and adiabatic wall. The grid utilized in this simulation is Cartesian with 401 nodes in the axial direction and 101 nodes in the vertical direction (except for a grid convergence study discussed in the following text). The geometry and flow conditions for this case are chosen as representative of a realistic scramjet flow. The specific injection conditions are selected to examine the effect on fuel-air mixing of closely matching the fuel velocity, pressure, and injection angle to that of the local (turned) flow at the inlet shoulder. It is expected that the additional penetration driven by such a selection might result in an increased mixing rate. Note, however, that rapid fuel-air mixing in real scramjet combustors must, in general, rely on three-dimensional effects such as vortex generation from ramp structures.^{6,7} The two-dimensional geometry and resulting flowfield shown in this work are selected primarily to demonstrate the application of the thrust modeling techniques discussed in previous sections. From the second-law standpoint, this flow is highly complex with all the relevant features of a three-dimensional simulation, i.e., embedded shocks, mixing and reaction, viscous effects, and heat transfer between streamtubes.

The computations are performed utilizing a two-dimensional version of the time-accurate Navier-Stokes code, SPARK, developed at NASA Langley Research Center.⁸ This code has been previously and extensively validated for mixing and reacting high-speed flows. A seven-reaction, seven-species (H_2 , O_2 , H_2O , OH , H , O , N_2) finite rate kinetics model is utilized in this work to model H_2 -air chemistry. Species diffusion and thermal conduction are scaled by the calculated viscosity through the selection of the turbulent Schmidt and Prandtl numbers. In this study, both quantities are held constant at 0.5 in the combustor region, whereas the turbulent Prandtl number

is equal to 0.9 everywhere in the inlet. The turbulent viscosity for the solution presented here is generated utilizing a simple algebraic scheme, modified to include injection effects.⁴ More accurate predictions of turbulence diffusion quantities are desirable for future detailed studies of thrust-performance losses in engine flowfields utilizing the techniques introduced in this work. The flowfield in this study is time-averaged over an appropriate number of iterations (once minimal convergence requirements are met) to ensure a steady flowfield approximation for use in the second-law analysis presented next.

Figure 8 shows both predicted hydrogen mass fraction contours and pressure contours in this flow. The oblique shock reflects from the top boundary and impinges upon the hydrogen jet near the injector itself. The effect of the shock on the fuel plume is to pinch the fuel, such that the fueled region flattens noticeably along the wall. The interaction of the plume with the reflected shock effectively destroys the reflected inlet shock; subsequent weaker shock structures downstream are caused primarily by flow recompression behind the expansion over and behind the fuel jet. Figure 9 plots mixing efficiency and combustion efficiency vs axial distance along the combustor. Mixing efficiency is defined here as the ratio of the integrated mass flux of the least available reactant in water product if complete reaction occurred with no further mixing over the integrated mass flux of the least available reactant. It is a parameter that describes the degree of mixedness between fuel and oxidizer and varies between 0 and 1. Combustion efficiency is defined as the ratio of the mass flow rate of hydrogen actually associated with reaction-generated water to the total injected hydrogen mass flow rate. Both mixing and combustion are seen to be relatively low (as expected) for this two-dimensional flow. The combustion efficiency is about 4% lower than the mixing efficiency at the end of the computational domain because of the presence of intermediate species OH and H .

Figure 10 presents a complete summary of the cumulative irreversible entropy distribution in this flowfield as referenced from the inflow station. The overall irreversibility (entropy) is seen to increase monotonically; it is nearly linear in the inlet. The individual entropy gain associated with a particular loss mechanism is computed for each of the cells within the simulated flowfield; these values are then summed (for each particular loss) over all cells on the i th row of cells (i.e., between x and $x + dx$). The shock-induced irreversibility is then backed out at each axial position by simply subtracting the sum of all other entropy gains from the overall irreversible entropy increase. The primary contributor to the overall entropy gain in the inlet region is the oblique shock. Heat transfer irreversibility in the inlet is minimal, whereas the frictional contribution is significant. The combustor is seen in Fig. 10 to produce over 80% of the total irreversibility for this flowfield; this irreversibility is caused by friction, heat transfer, fuel-air mixing, finite rate kinetics, and the shock structures. Note that the vertical ordering of these loss mechanisms is arbitrary. Because

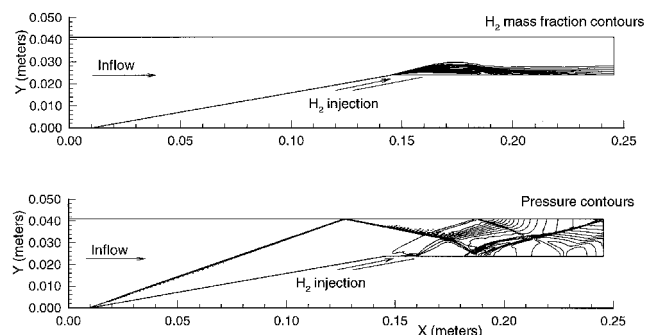


Fig. 8 Two-dimensional scramjet inlet and combustor (H_2 mass fraction and pressure contours).

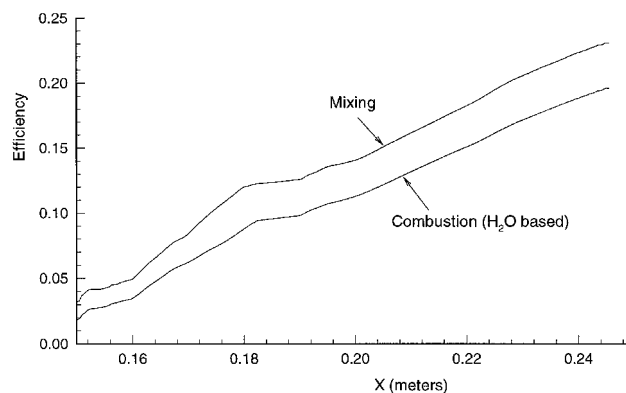


Fig. 9 Mixing and combustion efficiency vs axial distance.

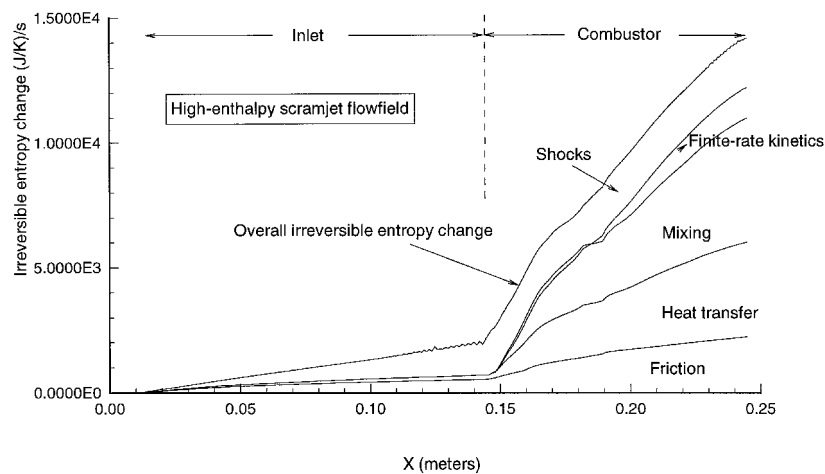


Fig. 10 Irreversible entropy axial distribution in two-dimensional scramjet inlet-combustor.

of the low relative temperature of the injected fuel, additional shearing between fuel and air, and the increased turbulence behind the jet, the rate of irreversible entropy increase caused by friction is seen to increase significantly in the combustor. Losses caused by heat transfer are driven mainly by temperature differences between the air and the jet, and increased turbulence and are observed to increase dramatically over similar losses in the inlet region. By the end of the combustor, the total cumulative heat transfer entropy increase is about 20% greater than the overall frictional increase. The mixing-induced entropy increase is associated solely with species diffusion, and yet represents the largest single irreversible increment in this flow. This is despite the low overall bulk mixing, as seen in Fig. 9. Both heat and mass diffusion are driven by the selection of the turbulent diffusion numbers (Prandtl and Schmidt numbers); the actual spatial distributions of these ratios are unknown at this time for such flows.

The entropy component caused by the finite rate reaction in Fig. 10 actually declines slightly near the jet (note the slight overlap between the finite rate and the mixing regions on this plot), but begins to increase significantly in the downstream region. It approaches the magnitude of the cumulative increase associated with the friction mechanism by the end of the domain. As discussed earlier, the entropy caused by an individual loss mechanism can actually decline in a complex flowfield with coupled losses; this effect, of course, must be countered by a corresponding (greater) increase in irreversible entropy caused by the other coupled loss mechanisms. Finally, the shock-induced irreversibility remains relatively constant across the combustor. However, this observation must be made in conjunction with the earlier discussion in which it was pointed out that some portion of shock losses may be automatically captured within the separate friction and heat transfer loss computations caused by spatial diffusion of the shocks across grid cells.

Figure 11 illustrates the effect of grid refinement on the computed cumulative irreversible entropy increases within the inlet. Entropy gain predictions using a grid with 201×101 nodes are compared to those for a 401×151 grid. Slight differences are seen in the individual entropy losses, although the overall entropy increase between the two grids is almost identical. This figure provides confidence that the computed loss mechanisms and subsequent lost thrust predictions are representative of a grid-converged scramjet combustor flowfield.

The stream thrust-potential distribution with associated thrust loss increment distributions is shown in Fig. 12 (for this flowfield) in which the reference area for all thrust-potential calculations is taken as the inlet area. The lowest curve on this figure represents the actual stream thrust availability through the flowfield. The actual thrust availability decreases in the inlet because of irreversibilities generated by shocks, heat

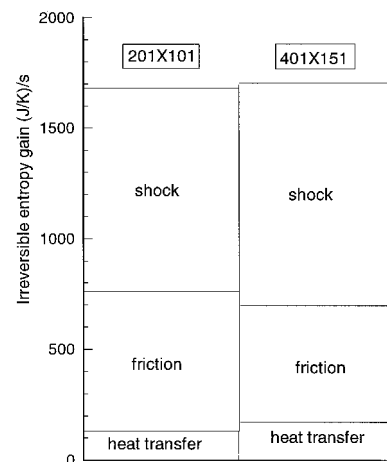


Fig. 11 Grid refinement effect on irreversibility in inlet.

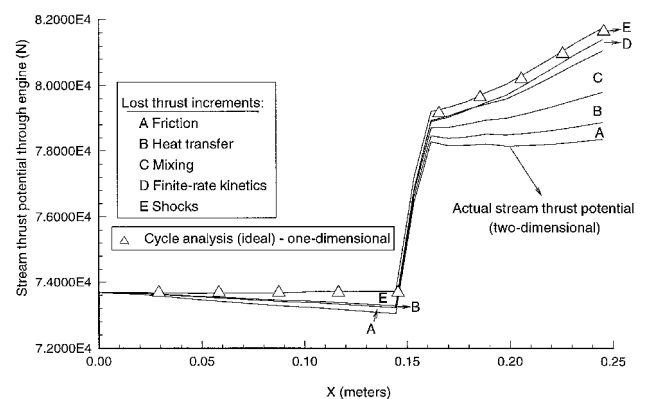


Fig. 12 Stream thrust potential and lost stream thrust potential increments vs axial distance in two-dimensional scramjet engine.

transfer between streamtubes, and viscous work between streamtubes and the boundary. The lost (or recovered) thrust increments in the inlet are similar in trend and relative magnitudes to the cumulative irreversible entropy increases shown in Fig. 10. In the inlet, the loss-corrected multidimensional thrust potential yields exactly the isentropic (one-dimensional) cycle predicted thrust potential, i.e., simply the inlet stream thrust itself.

Downstream-directed fuel injection takes place between $x = 0.1455$ m and $x = 0.16$ m and is responsible for the abrupt gain in thrust potential observed in that region in Fig. 12. The actual stream thrust availability is seen to decline slightly be-

cause of losses immediately after the injection and then begins to rise in the latter part of the combustor because of energy release associated with exothermic finite rate reactions. The lost thrust increments caused by various loss mechanisms within the combustor are similar (but not identical) in trends and relative differences to the entropy gains shown in Fig. 10 for that same region. The top line in Fig. 12 corresponds to the multidimensional flow with all irreversibilities removed (i.e., the thrust lost caused by irreversibilities is fully recovered). Also, plotted at various axial stations are thrust potential results for a cycle code simulation of the reversible engine. This simulation is independent of the multidimensional simulation, with the exception that the species mass fluxes from the CFD simulation are used to schedule the species distribution within the cycle code simulation. The cycle code results and the corrected (reversible) thrust potential calculated from the multidimensional simulation show excellent agreement. This establishes the relationship between the performance potential of a complex multidimensional flowfield and the cycle code predicted performance potential of the same flow. Ideally, this agreement should be exact; any discrepancies are caused mainly by either numerical issues within the CFD simulation itself or in approximations in the computations of the individual entropy changes caused by individual loss mechanisms (which are calculated on a cell-to-cell basis as a part of the foregoing analysis).

Conclusions

This investigation continues the development and application of a method for directly computing thrust losses in an aerospace engine in terms of irreversible entropy increases. The method is extended to allow the second-law-based performance assessment of multidimensional flowfields and provides a consistent link between performance assessment utilizing multidimensional numerical simulations and performance prediction utilizing one-dimensional cycle code simulations. Coupling between losses in realistic flows is fully accounted for by consistently applying the method while using the differential entropy axial distribution for the engine flowfield. The design of mission-optimized high-speed vehicles requires detailed understanding of performance loss mechanisms

within the engine; this and related investigations provide techniques for contributing to this understanding. Although this method for evaluating thrust losses is useful for any Brayton cycle engine, it should be particularly useful for high-speed engines for both quantitative evaluation and fundamental understanding of the physics of mixing enhancement strategies as well as in parametric engine design studies.

Acknowledgments

This work was performed under NASA Grant NAG1-1189 from NASA Langley Research Center (Hypersonic Vehicle Office). Special thanks go to Charles McClinton, Dennis Bushnell, Paul Vitt, Phil Drummond, Clay Rogers, Aaron Auslender, and Griff Anderson for many instructive conversations and suggestions over the course of several years concerning the topics discussed in this work.

References

- ¹Riggins, D. W., McClinton, C. R., and Vitt, P. H., "Thrust Losses in Hypersonic Engines Part 1: Methodology," *Journal of Propulsion and Power*, Vol. 13, No. 2, 1997, pp. 281–287.
- ²Clarke, J. M., and Horlock, J. H., "Availability and Propulsion," *Journal of Mechanical Engineering Science*, Vol. 17, No. 4, 1975, pp. 223–232.
- ³Lewis, J. H., "Propulsive Efficiency from an Energy Utilization Standpoint," *Journal of Aircraft*, Vol. 13, No. 4, 1976, pp. 299–302.
- ⁴Riggins, D. W., McClinton, C. R., Rogers, R. C., and Bittner, R. D., "Investigation of Scramjet Injection Strategies for High Mach Number Flows," *Journal of Propulsion and Power*, Vol. 11, No. 3, 1995, pp. 409–418.
- ⁵Murthy, S. N. B., "Effectiveness of a Scram Engine," AIAA Paper 94-3087, June 1994.
- ⁶Drummond, J. P., Carpenter, M. H., and Riggins, D. W., "Mixing and Mixing Enhancement in Supersonic Reacting Flowfields," *High-Speed Flight Propulsion Systems*, edited by S. N. B. Murthy and E. T. Curran, Vol. 137, Progress in Astronautics and Aeronautics, AIAA, Washington, DC, 1991, pp. 383–455.
- ⁷Riggins, D. W., and Vitt, P. H., "Vortex Generation and Mixing in Three-Dimensional Supersonic Combustors," *Journal of Propulsion and Power*, Vol. 11, No. 3, 1995, pp. 419–426.
- ⁸Drummond, J. P., Rogers, R. C., and Hussaini, M. V., "A Detailed Numerical Model of a Supersonic Reacting Mixing Layer," AIAA Paper 86-1427, June 1986.